

# A Novel Imaging Marker for Small Vessel Disease Based on Skeletonization of White Matter Tracts and Diffusion Histograms

Ebru Baykara, MSc,<sup>1</sup> Benno Gesierich, PhD,<sup>1</sup> Ruth Adam, PhD,<sup>1</sup>  
 Anil Man Tuladhar, MD,<sup>2</sup> J. Matthijs Biesbroek, MD, PhD,<sup>3</sup>  
 Huiberdina L. Koek, MD, PhD,<sup>4</sup> Stefan Ropele, PhD,<sup>5</sup> Eric Jouvent, MD, PhD,<sup>6,7,8</sup>  
 Alzheimer's Disease Neuroimaging Initiative, Hugues Chabriat, MD, PhD,<sup>6,7,8</sup>  
 Birgit Ertl-Wagner, MD,<sup>9</sup> Michael Ewers, PhD,<sup>1</sup> Reinhold Schmidt, MD,<sup>5</sup>  
 Frank-Erik de Leeuw, MD, PhD,<sup>2</sup> Geert Jan Biessels, MD, PhD,<sup>3</sup>  
 Martin Dichgans, MD,<sup>1,10,11</sup> and Marco Duering, MD<sup>1</sup>

**Objective:** To establish a fully automated, robust imaging marker for cerebral small vessel disease (SVD) and related cognitive impairment that is easy to implement, reflects disease burden, and is strongly associated with processing speed, the predominantly affected cognitive domain in SVD.

**Methods:** We developed a novel magnetic resonance imaging marker based on diffusion tensor imaging, skeletonization of white matter tracts, and histogram analysis. The marker (peak width of skeletonized mean diffusivity [PSMD]) was assessed along with conventional SVD imaging markers. We first evaluated associations with processing speed in patients with genetically defined SVD ( $n = 113$ ). Next, we validated our findings in independent samples of inherited SVD ( $n = 57$ ), sporadic SVD ( $n = 444$ ), and memory clinic patients with SVD ( $n = 105$ ). The new marker was further applied to healthy controls ( $n = 241$ ) and to patients with Alzheimer's disease ( $n = 153$ ). We further conducted a longitudinal analysis and interscanner reproducibility study.

**Results:** PSMD was associated with processing speed in all study samples with SVD ( $p$ -values between  $2.8 \times 10^{-3}$  and  $1.8 \times 10^{-10}$ ). PSMD explained most of the variance in processing speed ( $R^2$  ranging from 8.8% to 46%) and consistently outperformed conventional imaging markers (white matter hyperintensity volume, lacune volume, and brain volume) in multiple regression analyses. Increases in PSMD were linked to vascular but not to neurodegenerative disease. In longitudinal analysis, PSMD captured SVD progression better than other imaging markers.

**Interpretation:** PSMD is a new, fully automated, and robust imaging marker for SVD. PSMD can easily be applied to large samples and may be of great utility for both research studies and clinical use.

ANN NEUROL 2016;80:581–592

View this article online at [wileyonlinelibrary.com](http://wileyonlinelibrary.com). DOI: 10.1002/ana.24758

Received Feb 5, 2016, and in revised form Aug 8, 2016. Accepted for publication Aug 9, 2016.

Address correspondence to Dr Duering, Institute for Stroke and Dementia Research, Feodor-Lynen-Str 17, 81377 Munich, Germany.  
 E-mail: [marco.duering@med.uni-muenchen.de](mailto:marco.duering@med.uni-muenchen.de)

From the <sup>1</sup>Institute for Stroke and Dementia Research, Klinikum der Universität München, Ludwig-Maximilians-University LMU, Munich, Germany; <sup>2</sup>Radboud University Medical Center, Donders Institute for Brain, Cognition, and Behavior, Department of Neurology, Nijmegen, the Netherlands; <sup>3</sup>Department of Neurology, Brain Center Rudolf Magnus, University Medical Center Utrecht, Utrecht, the Netherlands; <sup>4</sup>Department of Geriatrics, University Medical Center Utrecht, Utrecht, the Netherlands; <sup>5</sup>Department of Neurology, Medical University of Graz, Graz, Austria; <sup>6</sup>Université Paris Diderot, Sorbonne Paris Cité, UMR-S 1161 National Institute for Health and Medical Research (INSERM), Paris, France; <sup>7</sup>Departement Hospitalo-Universitaire NeuroVasc Sorbonne Paris Cité, Paris, France; <sup>8</sup>Department of Neurology, Lariboisière Hospital, Assistance Publique - Hôpitaux de Paris, Paris, France; <sup>9</sup>Institute of Clinical Radiology, Klinikum der Universität München, Ludwig-Maximilians-University LMU, Munich, Germany; <sup>10</sup>Munich Cluster for Systems Neurology (SyNergy), Munich, Germany; and <sup>11</sup>German Center for Neurodegenerative Diseases (DZNE), Munich, Germany.

A complete listing of Alzheimer's Disease Neuroimaging Initiative investigators can be found at: [http://adni.loni.usc.edu/wp-content/uploads/how\\_to\\_apply/ADNI\\_Acknowledgement\\_List.pdf](http://adni.loni.usc.edu/wp-content/uploads/how_to_apply/ADNI_Acknowledgement_List.pdf)

Additional supporting information can be found in the online version of this article.

Cerebral small vessel disease (SVD) represents a major cause of vascular cognitive impairment (VCI) and dementia, either by its own or in combination with neurodegenerative pathology.<sup>1</sup> Progress in understanding and managing SVD has been relatively slow. This in part relates to the lack of a good disease marker that is quantitative and robust, reflects disease burden, and can easily be applied to a large number of subjects.

Previous studies have suggested a wide range of mostly magnetic resonance imaging (MRI)-based markers for SVD and VCI. The most commonly used markers are white matter hyperintensity (WMH) and lacune volumes.<sup>2</sup> However, both markers have clear limitations. First, lesion quantification is labor-intensive and subject to bias because of errors in lesion classification and the requirement for manual corrections.<sup>3</sup> Second, associations with clinical symptoms, such as cognitive deficits, are typically weak.<sup>4,5</sup> Stronger associations have been reported for brain volume.<sup>4,6,7</sup> However, alterations in brain volume are relatively unspecific and generally considered a marker for neurodegenerative pathology.<sup>8</sup> Also, automated volumetric analysis of diseased brains is methodologically challenging because of altered tissue contrast.<sup>9,10</sup> Hence, there is great demand for better markers of SVD burden.<sup>2,11,12</sup>

Diffusion tensor imaging (DTI) is a sensitive technique that allows quantifying microstructural tissue alterations,<sup>13</sup> which can be invisible on conventional MRI. The typical pattern of diffusion change in SVD is a reduction in directionality, as captured by fractional anisotropy (FA), and a prominent increase in the magnitude of diffusion, as captured by mean diffusivity (MD). Previous studies suggested that these DTI metrics are superior to conventional imaging markers in assessing disease burden in SVD.<sup>4,14,15</sup> However, there are obstacles to the wider application of DTI measures, in particular, the need for extensive data postprocessing such as the removal of prominent cerebrospinal fluid (CSF) signal from MD images.

The aim of this study was to develop a new imaging marker for disease burden in SVD that can be used in clinical routine and readily applied to large samples. We requested that this marker should reflect the underlying disease (SVD) and correlate with clinical deficits typically seen in these patients. We further reasoned that the marker should be robust, fully automated, and easy to implement. To this end, we combined 2 processing techniques for DTI data: skeletonization and histogram analysis. Skeletonization focuses the analysis of MD on the main fiber tracts, thereby largely eliminating CSF contamination. Whole brain histogram analysis is particularly appropriate when dealing with diffuse diseases and when quantifying total disease burden.<sup>16</sup>

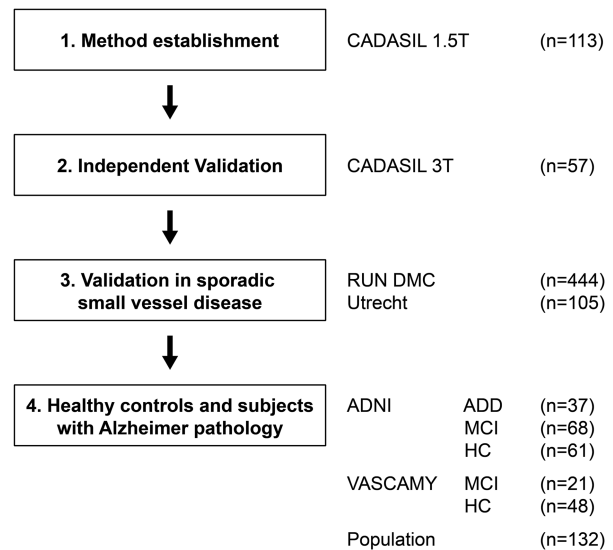


**FIGURE 1: Study design.** The new imaging marker peak width of skeletonized mean diffusivity (PSMD) was first established in a large CADASIL data set with magnetic resonance imaging at 1.5T. Independent validation was performed in a new CADASIL sample scanned at 3T. In a third step, the marker was applied to samples with sporadic small vessel disease (RUN DMC and Utrecht). Lastly, the marker was evaluated in healthy subjects (HC) as well as samples with predominant Alzheimer pathology (mild cognitive impairment [MCI] and Alzheimer's disease dementia [ADD]). Numbers indicate subjects with usable diffusion tensor imaging data in the samples.

We first established our new imaging marker, peak width of skeletonized mean diffusivity (PSMD), in patients with cerebral autosomal-dominant arteriopathy with subcortical infarcts and leukoencephalopathy (CADASIL), a genetically defined form of severe SVD. We analyzed the relationship of this marker with processing speed, because speed has emerged as the most prominently affected cognitive domain in SVD. Next, we validated our results in an independent sample of CADASIL patients. We then evaluated 2 samples comprising patients with sporadic SVD. In each sample, we compared PSMD with conventional SVD markers. We also applied the novel marker to healthy controls and patients with Alzheimer's disease (AD) pathology (Fig 1). Finally, we addressed the utility of the new marker in multicenter trials through sample size estimations and assessment of interscanner reproducibility.

## Subjects and Methods

### Subjects, MRI Acquisition, and Neuropsychological Testing

All studies used in this analysis were approved by the ethics committees of the respective institutions. Written informed consent was obtained from all subjects. Characteristics of the study samples are provided in Tables 1 and 2.

**TABLE 1. Characteristics of Study Samples with Predominant Vascular Disease**

Characteristic	CADASIL Exploratory, n = 113	CADASIL Validation (VASCAMY), n = 57	Sporadic SVD (RUN DMC), n = 444	Memory Clinic Patients with SVD (Utrecht), n = 105
Demographic characteristics				
Age, yr, mean (SD) [min, max]	49.1 (9.5) [22.9, 72.8]	53.4 (10.7) [29.0, 72.0]	65.3 (8.9) [49.6, 85.5]	74.9 (8.3) [50.0, 92.0]
Education, yr, mean (SD) [min, max]	10.5 (2.2) [9, 16]	14 (2.7) [10, 20]	11 (3.6) [4, 19]	12.2 (2.7) [4, 17]
Female, No. {%}	61 {54.0}	19 {33.3}	201 {45.3}	51 {48.6}
Vascular risk factors, No. {%}				
Current smoker	28 {24.8}	11 {19.3}	69 {15.5}	10 {9.5}
Past smoker	39 {34.5}	24 {42.1}	239 {53.8}	57 {54.3}
Hypertension	26 {23.0}	13 {22.8}	320 {72.1}	97 {92.4}
Hypercholesterolemia	36 {31.9}	24 {42.1}	194 {43.7}	64 {61.0}
Diabetes	0 {0.0}	0 {0.0}	61 {13.7}	29 {27.6}
Cognitive scores				
TMT-A, <sup>a</sup> median (IQR) [min, max]	-0.85 (2.64) [-22.22, 1.39]	-0.50 (1.61) [-13.24, 1.34]	—	-1.29 (3.03) [-13.05, 1.02]
TMT-B, <sup>a</sup> median (IQR) [min, max]	-2.14 (4.60) [-16.38, 1.67]	-0.48 (3.05) [-11.59, 1.72]	—	-1.73 (3.05) [-22.11, 1.51]
1-letter P&P MST, <sup>a</sup> median (IQR) [min, max]	—	—	-2.91 (2.71) [-17.97, 1.45]	—
LDST, <sup>a</sup> median (IQR) [min, max]	—	—	-0.38 (2.15) [-3.74, 4.47]	—
Speed score, <sup>a</sup> median (IQR) [min, max]	-1.56 (2.80) [-17.44, 1.24]	-0.56 (2.33) [-12.42, 1.16]	-1.67 (2.17) [-10.20, 2.96]	-1.73 (2.60) [-11.52, 1.13]
MMSE, median (IQR) [min, max]	29 (3) [15, 30]	30 (1) [22, 30]	29 (2) [22, 30]	26 (4) [20, 30]
Imaging characteristics				
PSMD, 10 <sup>-4</sup> mm <sup>2</sup> /s, median (IQR) [min, max]	5.43 (2.92) [2.82, 10.87]	5.47 (2.69) [2.63, 9.47]	3.28 (0.87) [2.30, 7.95]	4.24 (1.05) [2.82, 8.72]
Normalized WMHV, %, median (IQR) [min, max]	9.81 (8.80) [0.06, 30.99]	7.38 (7.53) [0.09, 22.84]	0.59 (1.23) [0.05, 14.03]	1.12 (2.58) [0, 7.70]
Normalized LV, %, median (IQR) [min, max]	0.0093 (0.0315) [0, 0.2118]	0.0240 (0.0639) [0, 0.2477]	0 (0) [0, 0.1027]	0 (0) [0, 0.0577]
BPF, median (IQR) [min, max]	0.836 (0.068) [0.655, 0.935]	0.784 (0.069) [0.699, 0.872]	0.654 (0.077) [0.499, 0.809]	0.621 (0.055) [0.528, 0.759]

<sup>a</sup>Age and education adjusted z scores.

BPF = brain parenchymal fraction; IQR = interquartile range; LDST = Letter-Digit Substitution Task; LV = lacune volume; MMSE = Mini-Mental State Examination; P&P MST = Paper-Pencil Memory Scanning Test; PSMD = peak width of skeletonized mean diffusivity; SD = standard deviation; SVD = small vessel disease; TMT = Trail Making Test; WMHV = white matter hyperintensity volume.

**CADASIL EXPLORATORY SAMPLE.** The novel DTI-based marker was developed in an exploratory sample of 117 patients with CADASIL from a previous, prospective study.<sup>17</sup> The diagnosis was confirmed either by genetic testing or skin biopsy. Four patients were excluded due to insufficient quality of the DTI images. For the regression analysis on processing speed, additional 9 subjects were excluded because of missing neuropsychological data. Therefore, the final sample for regression analyses consisted of 104 patients.

MRI scans were performed on a 1.5T Signa scanner (GE Healthcare, Solingen, Germany). Acquisition parameters are presented in Supplementary Table e-1.

Neuropsychological testing was performed on the previous or the same day as the MRI examination. Trail Making Test (TMT) matrix A and B were used to create a compound processing speed score. Raw test scores were transformed into age- and education-corrected *z* scores based on values from healthy subjects.<sup>18</sup>

Longitudinal data (follow-up at 18 months) were available for 58 patients.

**CADASIL VALIDATION SAMPLE (VASCAMY STUDY).** A total of 57 patients with CADASIL from the ongoing, prospective VASCAMY (Vascular and Amyloid Predictors of Neurodegeneration and Cognitive Decline in Nondemented Subjects) study were included in the validation sample. Again, the diagnosis was confirmed by either genetic testing or skin biopsy. From the same study, we also included 69 non-CADASIL subjects: 21 diagnosed

with (mostly amnesic) mild cognitive impairment and 48 healthy controls.

MRI scans were performed on a 3T Magnetom Verio scanner (Siemens, Erlangen, Germany). For interscanner reproducibility analysis, 7 CADASIL patients from the VASCAMY study were scanned back to back on both the 3T scanner and a 1.5T Siemens Magnetom Aera scanner. Acquisition parameters are presented in Supplementary Table e-1.

Neuropsychological testing was performed on the previous or the same day as the MRI examination. Similar to the exploratory sample, age- and education-corrected TMT A and B *z* scores were used to create a compound processing speed score.

**SPORADIC SVD SAMPLE (RUN DMC STUDY).** Four hundred forty-four subjects from the RUN DMC (Radboud University Nijmegen Diffusion Tensor and Magnetic Resonance Imaging Cohort) study<sup>19</sup> were included. The processing speed scores could not be calculated for 5 subjects because of missing neuropsychological data. Furthermore, 3 outliers were excluded from the regression analyses (see Statistical Analysis); the final sample for regression analysis consisted of 436 subjects.

MRI scans were performed on a 1.5T Siemens Magnetom Sonata scanner. Acquisition parameters are presented in Supplementary Table e-1.

Neuropsychological testing was performed within 3 weeks before the scanning. The 1-letter subtask of the Paper-Pencil Memory Scanning Test and the Letter-Digit Substitution Task were used to create a compound processing speed score. Raw

**TABLE 2. Characteristics of Healthy Controls and Patients with Alzheimer's Disease Pathology**

Characteristic	HC (VASCAMY), n = 48	MCI (VASCAMY), n = 21	HC (ADNI), n = 61	MCI (ADNI), n = 68	ADD (ADNI), n = 37	Population (ASPFS), n = 132
Demographic characteristics						
Age, yr, mean (SD) [min, max]	71.5 (6.3) [60, 84]	76.5 (4.4) [70, 87]	72.9 (5.7) [60.4, 87]	74.7 (8.1) [48.7, 88.6]	74 (8.2) [55.9, 90.2]	66.9 (11.4) [40, 85]
Education, yr, mean (SD) [min, max]	14 (3.1) [8, 20]	14 (3.7) [7, 20]	16.5 (2.8) [12, 20]	15.9 (2.7) [11, 20]	15 (2.8) [11, 20]	11.4 (2.8) [9, 18]
Female, No. {%}	30 {62.5}	11 {52.4}	37 {60.7}	24 {35.3}	12 {32.4}	81 {61.4}
Global cognitive score						
MMSE, median (IQR) [min, max]	30 (1) [27, 30]	27 (3) [22, 30]	29 (2) [24, 30]	27 (3) [23, 30]	23 (3) [15, 27]	28 (1) [23, 30]
Imaging						
PSMD, 10 <sup>-4</sup> mm <sup>2</sup> /s, median (IQR) [min, max]	3.05 (0.47) [2.58, 4.96]	3.33 (0.62) [2.72, 5.37]	3.02 (0.72) [2.23, 6.85]	3.20 (0.88) [2.35, 5.03]	3.47 (0.96) [2.59, 5.03]	3.05 (0.72) [2.16, 6.76]

ADD = Alzheimer's disease dementia; ASPFS = Austrian Stroke Prevention Family Study (comprising healthy elderly from the population); HC = healthy control; IQR = interquartile range; MCI = mild cognitive impairment; MMSE = Mini-Mental State Examination; PSMD = peak width of skeletonized mean diffusivity; SD = standard deviation.

test scores were transformed into age- and education-corrected  $z$  scores based on values from healthy subjects.<sup>20,21</sup>

**MEMORY CLINIC PATIENTS WITH SVD (UTRECHT).** One hundred thirty-three subjects from the Memory Clinic cohort of the Utrecht Vascular Cognitive Impairment Study Group were included. Recruitment and data collection were done according to the multicenter Dutch Parelinoer Institute neurodegenerative diseases protocol.<sup>22</sup> Twenty-three subjects had to be excluded due to motion slice artifacts in the DTI data. Five subjects had missing structural MRI data (T1, fluid-attenuated inversion recovery [FLAIR], or both) and were therefore not included in further analyses. Of the remaining 105 patients, 10 presented with subjective cognitive complaints, 43 with mild cognitive impairment (according to the Peterson criteria),<sup>23</sup> and 52 with dementia. To focus on patients with SVD within the memory clinic sample, we performed a prespecified subgroup analysis; subgroups were predefined according to the WMH load by splitting at the median normalized WMH volume. Subgroups consisted of 52 subjects with low WMH load and 53 with high WMH load. Three subjects from the low WMH and 6 subjects from the high WMH group had to be excluded from regression analyses because of missing cognitive data.

MRI scans were performed on an Intera 3T scanner (Philips, Best, the Netherlands). Acquisition parameters are presented in Supplementary Table e-1.

Neuropsychological testing was performed on the same day as the MRI examination. Similar to the CADASIL samples, age- and education-corrected TMT A and B  $z$  scores were used to create a compound processing speed score (mean of both  $z$  scores).

**ALZHEIMER'S DISEASE NEUROIMAGING INITIATIVE STUDY.** The Alzheimer's Disease Neuroimaging Initiative (ADNI) was launched in 2003 as a public-private partnership, led by Principal Investigator Michael W. Weiner, MD (for up-to-date information, see [www.adni-info.org](http://adni-info.org)). One hundred eighty-five subjects from the ADNI database (<http://adni.loni.usc.edu/>; from 17 centers with the same DTI protocol, ADNIGO and ADNI2 phases) were included in the current study. Nineteen subjects were excluded due to either missing diagnosis, missing MRI data, or motion artifacts in the DTI data. The final sample consisted of 166 subjects, of whom 61 were healthy controls, 68 were amnesic mild cognitive impairment (MCI) subjects, and 37 were AD dementia patients (diagnosis according to the National Institute of Neurological and Communication Disorders, Alzheimer's Disease and Related Disorders Association criteria for probable AD as outlined in the ADNI protocol).

MRI scans were performed on 3T GE Healthcare scanners (Signa HDxt and Discovery MR750). Acquisition parameters are presented in Supplementary Table e-1.

**AUSTRIAN STROKE PREVENTION FAMILY STUDY.** One hundred thirty-five community-dwelling, healthy subjects with DTI data were included from the Austrian Stroke Prevention Family Study (ASPF; Department of Neurology, Medical University Graz).<sup>24</sup> Three subjects were excluded due to insufficient

data quality of the DTI images. The final sample consisted of 132 subjects.

MRI scans were performed on a 3T Siemens Magnetom Tim Trio scanner. Acquisition parameters are presented in Supplementary Table e-1.

### MRI Processing

**DTI.** After a quick (maximum = 15 seconds) visual inspection to exclude the presence of major artifacts, diffusion-weighted images were corrected for eddy current-induced distortions and subject motion with the `eddy_correct` tool of the Functional Magnetic Resonance Imaging of the Brain (FMRIB) software library (FSL; v5.0).<sup>25</sup> In RUN DMC, diffusion data were pre-processed using the in-house-developed iteratively reweighted-least-squares algorithm PATCH.<sup>26</sup> After brain tissue extraction using BET (FSL), diffusion tensors and scalar diffusion parameters (ie, FA and MD) were calculated using DTIFIT (FSL).

**PSMD.** Fully automated calculation of the new marker comprised 2 steps: skeletonization of DTI data and histogram analysis (Fig 2). All study samples were processed through the same pipeline. First, DTI data were skeletonized using the Tract-Based Spatial Statistics procedure,<sup>27</sup> part of FSL. For this purpose, all subjects' FA data were aligned into a common space using the nonlinear registration tool FNIRT and the standard space FMRIB 1mm FA template. Each subject's FA data were then projected onto the skeleton, which was derived from the standard space template thresholded at an FA value of 0.2. Finally, MD images were projected onto the skeleton, using the FA-derived projection parameters. The final MD skeletons were further masked with the template skeleton thresholded at an FA value of 0.3 to avoid contamination of the skeleton through CSF partial volume effects. For the same reason, regions of the skeleton directly adjacent to the ventricles, such as the fornix, were removed from further analysis by a custom-made mask. The same template skeleton and mask were used for each study sample.

The new marker, PSMD, was calculated as the difference between the 95th and 5th percentiles of the voxel-based MD values within the skeleton (see Fig 2). We compared PSMD to established MD parameters (mean, median, peak height, full width at half maximum) in the exploratory CADASIL sample; PSMD showed the strongest association with processing speed scores and was therefore used for all subsequent analyses in all study samples.

A shell script for the calculation of PSMD is available at <http://www.psm-marker.com/>. The total calculation for 1 subject (from DTI raw data) takes approximately 12 minutes on a standard desktop computer. All processing steps (including pre-processing) are included in the shell script. No human intervention (eg, visual inspection or manual edits) is needed during or after the processing pipeline.

For comparison, we also calculated whole brain MD peak height, an established histogram measure for nonskeletonized data. First, CSF was removed by a conventional method (ie, intensity thresholding with a value of 0.0025). Next, the peak

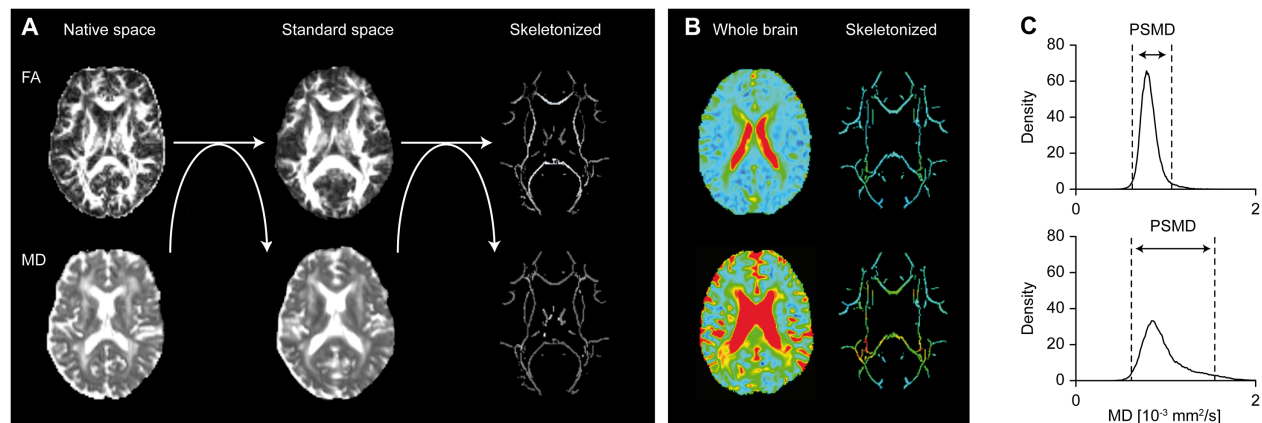


**FIGURE 2:** Procedure for marker calculation: skeletonization and histogram analysis. (A) Illustration of the automated skeletonization procedure. Individual fractional anisotropy (FA) images are normalized to standard space and projected onto the skeleton template. Next, the transformation and skeleton projection parameters are applied to the mean diffusivity (MD) images. (B) Examples of MD maps from 2 CADASIL subjects (upper and lower panel) projected onto the standard skeleton. (C) Histogram analysis of the same MD data as in B. Peak width of skeletonized MD (PSMD) is calculated as the difference between the 95th and 5th percentiles.

height of the histogram was estimated using the density function in R (v3.1.2)<sup>28</sup> and normalized by the total number of voxels in the histogram.

**NORMALIZED BRAIN VOLUME.** In each sample, brain parenchymal fraction (BPF; ie, normalized brain volume) was calculated by dividing the whole brain volume by intracranial cavity volume.

For the CADASIL exploratory sample and the RUN DMC study, the brain volume calculation procedure has already been described.<sup>6,15</sup> Due to uncorrectable failure in either brain or intracranial segmentation, we could not calculate BPF for 2 CADASIL subjects.

In the VASCAMY study, native space T1 and T2 images were segmented into tissue probability maps using the Statistical Parametric Mapping (SPM) toolbox (v12; Wellcome Department of Cognitive Neurology, London, UK; <http://www.fil.ion.ucl.ac.uk/spm>). For whole brain volume, T1 segmented gray matter and white matter tissue maps; and for the intracranial volume, T2 segmented gray matter, white matter, and CSF were combined, thresholded at 20%, and binarized. Manual editing was performed when necessary.

In the Utrecht study, native space T1 images and T2 images were segmented into tissue probability maps using SPM. For whole brain volume, T1 segmented gray matter and white matter tissue maps were combined, thresholded at 30%, and binarized. Intracranial volume was calculated using the BET (brain extraction) tool (FSL) on T2 images, and the resulting masks were manually edited if necessary.

**SUBCORTICAL LESION VOLUMES.** We used the STRIVE<sup>2</sup> criteria to define and identify WMHs and lacunes of presumed vascular origin. Detection and segmentation procedures have already been described for the CADASIL exploratory sample, the RUN DMC study, and the ADNI study.<sup>6,15,29</sup> Normalized WMH and lacune volumes for each sample were calculated by dividing through brain volume. For WMH volume in the

CADASIL validation (VASCAMY study) and Utrecht samples, bias-corrected 3-dimensional (3D) FLAIR images were first segmented into 3 tissue probability maps using the FAST tool from FSL. Next, WMHs were separated from CSF, which is located in the same tissue probability map, by histogram segmentation based on the Otsu method.<sup>30</sup> The WMH segmentations were then manually edited and cleaned from misclassified artifacts using a custom 3D editing tool.

To determine the lacune volume in the CADASIL validation and Utrecht samples, we used a seed-growing algorithm, implemented via an in-house software tool. After manually placing a seed voxel into a lacune on the 3D T1 image by an experienced rater, the tool tests all neighboring voxels for inclusion and repeats testing until no new voxels can be added. The inclusion criterion was the absolute intensity of the tested voxel and its intensity difference from the seed voxel. All cavities smaller than 3mm were ignored to exclude perivascular spaces.

**CEREBRAL MICROBLEEDS.** Using the STRIVE<sup>2</sup> criteria, cerebral microbleeds were identified and counted on T2\*-weighted gradient echo images by trained raters.

### Statistical Analysis

All statistical analyses were performed in R (v3.1.2).<sup>28</sup> The association between MRI parameters (PSMD, normalized WMH volume, normalized lacune volume, BPF, and microbleed count), age, sex, and the processing speed scores was evaluated by linear regression. The distributions of speed scores were tested for normality in each sample with the Shapiro-Wilk test, and scores were log transformed in case of non-normal distribution. To ensure that the regression results were not driven by outliers, they were identified with the Bonferroni outlier test (car R package, v2.0-25)<sup>31</sup> and excluded from regression analyses (only 3 subjects from the RUN DMC sample).

To identify the imaging marker with the highest relative importance, we included all markers into multiple linear

regression models and applied a model decomposition method described by Lindeman et al,<sup>32</sup> as implemented in the relaimpo R package (v2.2-2).<sup>33</sup> Additionally, we used stepwise backward regression with MRI parameters, age, and sex to identify independent associations with processing speed. The Akaike Information Criterion (AIC) was used to select the model with the best fit (minimized AIC value). All  $R^2$  values reported are adjusted  $R^2$  values. For group comparisons of PSMD across different clinical samples (within studies), we used the Wilcoxon rank sum test. To correct for multiple comparisons, Bonferroni-corrected p-values are reported for group comparisons. The sample size estimates were calculated on the longitudinal change of variables using the G\*Power tool<sup>34</sup> (difference between 2 independent means, 2-tailed, type I error rate = 0.05, power = 0.80). We used the raw change between baseline and follow-up data and hypothetical treatment effects of 10%, 20%, and 30%. Interscanner reproducibility was assessed by the intraclass correlation coefficient (ICC) as implemented in R.

## Results

Demographic, clinical, and MRI characteristics of the study samples with SVD are presented in Table 1. Details on study samples with healthy controls and subjects with AD diagnosis are presented in Table 2.

### Exploratory Analysis in CADASIL Patients

Linear regression (Supplementary Table e-2) revealed PSMD to have the strongest association with processing speed scores (Fig 3A, upper panel). Speed scores were further significantly associated with all other imaging markers and age (see Supplementary Table e-2). For comparison, we added an established DTI histogram marker (whole brain MD peak height), which explained less variance than PSMD.

Analysis of the relative importance of the regressors showed that PSMD contributed most to the multiple regression model (see Fig 3A, lower panel). To determine the best model, we further conducted a backward stepwise regression. PSMD and the normalized volumes of both WMH and lacunes were retained in the final model (see Supplementary Table e-2).

### Validation in Independent Samples

In the independent CADASIL validation sample, linear regression (see Supplementary Table e-2) revealed a strong association between PSMD and speed scores (see Fig 3B, upper panel). Speed scores were further significantly associated with microbleed count, normalized lacune volume, and age (see Supplementary Table e-2). Importantly, PSMD contributed most to the regression model (see Fig 3B, lower panel). For further exploration, we again conducted backward stepwise regression; PSMD and normalized lacune volume were retained in the final model.

To validate our findings in the more common, sporadic form of SVD, we next analyzed data from the RUN DMC study. Linear regression (see Supplementary Table e-2) showed a significant association between PSMD and speed scores (see Fig 3C, upper panel). Speed scores were also significantly associated with all other imaging markers, age, and sex (see Supplementary Table e-2). Again, PSMD contributed most to the multiple regression model (see Fig 3C, lower panel). Further exploratory backward stepwise regression resulted in a final model that included only PSMD.

We next extended our findings to sporadic SVD in a memory clinic setting (Utrecht study). None of the linear regression analyses with the MRI markers (PSMD, normalized WMH volume, lacune volume, BPF, and microbleed count) showed a significant association with the speed scores (not shown) within the entire memory clinic sample. In subjects with prominent vascular disease as determined by a WMH load above the median value (high WMH subgroup,  $n = 53$ ), we found a significant association (see Supplementary Table e-2) between PSMD and speed scores (see Fig 3D, upper panel). Speed scores were also significantly associated with age (see Supplementary Table e-2). Focusing on the low WMH load group ( $n = 52$ ), the only imaging variable that was significantly associated with speed scores was BPF ( $p = 0.023$ ,  $R^2 = 0.09$ ). Importantly, PSMD contributed most to the multiple regression model (see Fig 3D, lower panel). Further exploratory backward stepwise regression resulted in a final model that included PSMD and age.

### Comparison with Healthy Controls and Subjects with Alzheimer Pathology

Figure 4 demonstrates that patient samples with high SVD burden (CADASIL, RUN DMC, Utrecht) had higher PSMD compared with healthy controls and AD patients (MCI and AD dementia). Moreover, PSMD increased with higher WMH load. Focusing on the ADNI sample, there was no difference between healthy controls (PSMD median =  $3.020 \times 10^{-4} \text{mm}^2/\text{s}$ ) and MCI patients with low WMH load (median =  $2.935 \times 10^{-4} \text{mm}^2/\text{s}$ ,  $W = 903$ ,  $p = 1$ ) or AD dementia patients with low WMH load (median =  $3.415 \times 10^{-4} \text{mm}^2/\text{s}$ ,  $W = 477$ ,  $p = 1$ ). Also, healthy controls had comparable PSMD across studies: VASCAMY (median =  $3.045 \times 10^{-4} \text{mm}^2/\text{s}$ ), ADNI (median =  $3.020 \times 10^{-4} \text{mm}^2/\text{s}$ ), and population sample (ASPFs, median =  $3.045 \times 10^{-4} \text{mm}^2/\text{s}$ ).

There was no significant association between PSMD and processing speed in any of the non-SVD samples (p-values ranging between 0.24 and 0.79).

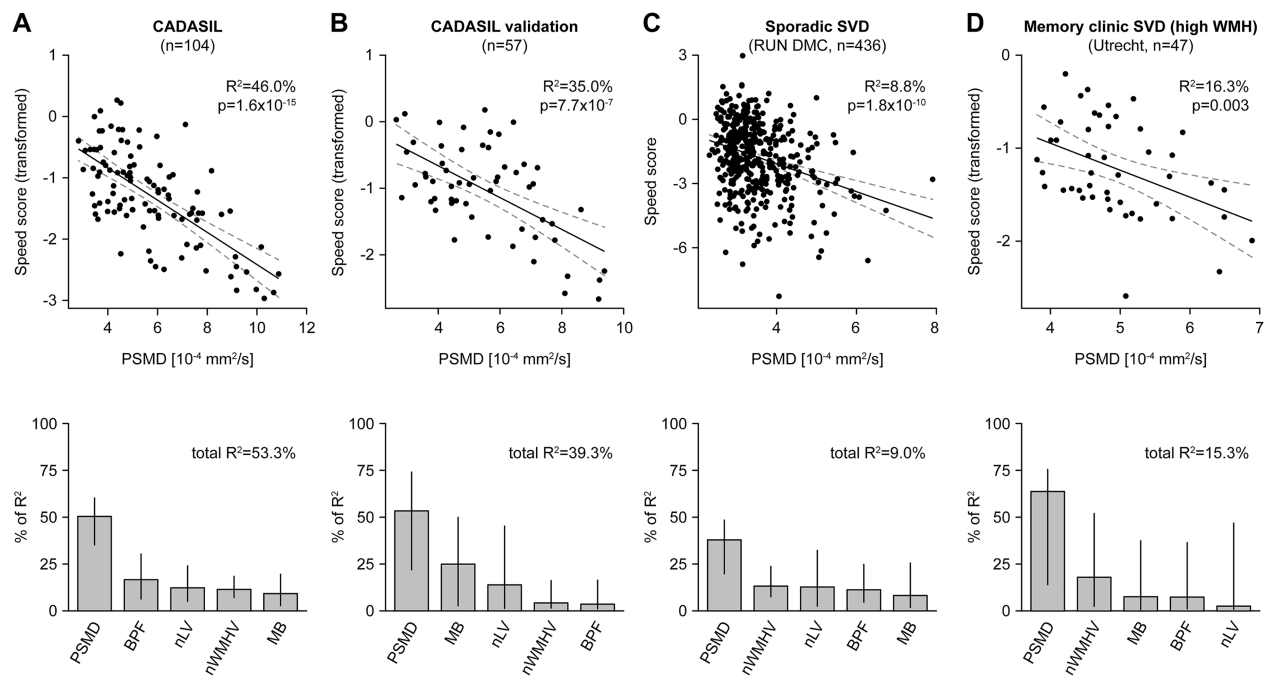


**FIGURE 3: Association between imaging markers and processing speed performance in small vessel disease (SVD).** Upper panels: Simple linear regression between peak width of skeletonized mean diffusivity (PSMD) and processing speed scores in (A) the exploratory CADASIL sample, (B) the CADASIL validation sample, (C) the sporadic SVD sample (RUN DMC), and (D) the memory clinic patients with SVD (Utrecht). Dashed lines indicate 95% confidence intervals for the regression. Lower panels depict the contribution of each regressor (PSMD, normalized white matter hyperintensity volume [nWMHV], normalized lacune volume [nLV], brain parenchymal fraction [BPF], and microbleed count [MB]) to the multiple regression models as estimated by the Lindeman–Merenda–Gold method. Note that in all cases PSMD contributes most to the models. Lines represent 95% confidence intervals after bootstrapping.

### Utility of PSMD for Clinical Trials

The longitudinal analysis of CADASIL patients from the exploratory sample (18 months of follow-up,  $n = 58$ ) showed a significant change for PSMD ( $p = 8.98 \times 10^{-13}$ , paired  $t$  test) and normalized WMH volume ( $p = 2.21 \times 10^{-6}$ ), but not for other imaging markers ( $p$ -values between 0.197 and 0.423) or the processing speed score ( $p = 0.260$ ). Power calculations revealed the smallest sample size estimate for PSMD (Table 3).

To address the utility in multicenter studies, we conducted an interscanner reproducibility study in 7 CADASIL patients using 2 scanners with different field strengths (3T and 1.5T). Reproducibility was highest for PSMD (ICC = 0.948) and considerably lower for other MD measures, such as the traditional histogram measure whole brain MD peak height (ICC = 0.752) or more simple measures: average of skeletonized MD (ICC = 0.730) and median of skeletonized MD (ICC = 0.691).

### Discussion

Our study establishes a novel imaging marker for SVD. This marker combines DTI, skeletonization of white matter tracts, and the analysis of MD histograms. Calculation of this marker is fully automated, fast, and robust, thus fulfilling the requirements for routine use and

application to large samples. PSMD explained a substantial proportion of variance in processing speed, the predominantly affected cognitive domain in SVD, and consistently outperformed other imaging markers for SVD. We could validate our findings in independent samples of SVD. We further found this marker to be linked to small vessel pathology but not to neurodegenerative pathology. Finally, PSMD showed the smallest sample size estimate in the longitudinal analysis and the highest interscanner reproducibility. We thus consider PSMD to be of great value for research studies and potentially also for use in clinical routine and trials.

A major finding of our study is the strong association between PSMD and deficits in processing speed across all study samples including patients with genetically defined SVD, patients with sporadic SVD, and memory clinic patients with high WMH burden. The association was strongest for patients with inherited SVD, who on average were the most severely affected group as judged by the normalized volume of WMH, the normalized volume of lacunes, and PSMD. Although the association was weaker for patients with sporadic SVD, PSMD consistently showed the strongest contribution to processing speed impairment when compared with other imaging markers. Importantly, as judged by

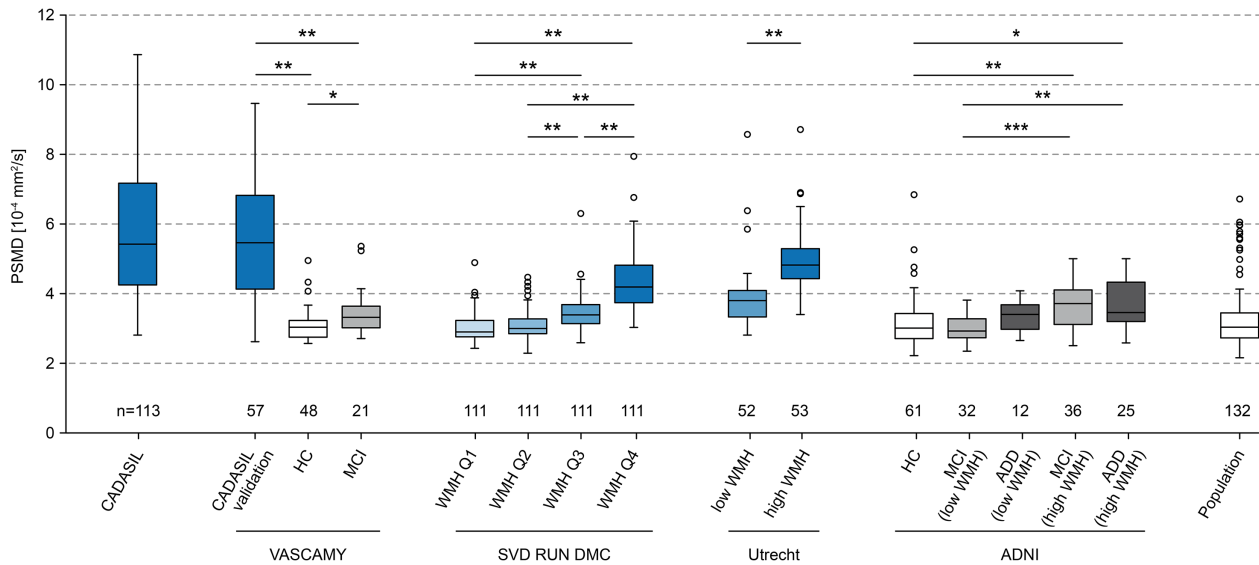


**FIGURE 4: Peak width of skeletonized mean diffusivity (PSMD) in subjects with small vessel disease (SVD), healthy controls (HC), and subjects with Alzheimer’s disease (AD). PSMD is presented across samples: CADASIL, sporadic SVD (RUN DMC, Utrecht), mild cognitive impairment (MCI; VASCAMY and ADNI), and AD dementia (ADD; ADNI). RUN DMC, Utrecht, and ADNI samples were split into subgroups based on the volume of white matter hyperintensities (WMH; according to median split or quartiles [Q]). Group comparisons were calculated between subgroups within studies: \*p < 0.05, \*\*p < 0.01, \*\*\*p < 0.001 (Wilcoxon rank sum tests after Bonferroni correction). Samples selected on the basis of SVD pathology are indicated in blue. Samples selected on the basis of AD-typical cognitive deficits are indicated in gray.**

stepwise regression analyses, PSMD was the only imaging marker showing an independent association with processing speed in every SVD sample.

Methodological challenges in quantifying disease burden have been a major roadblock to research on SVD and related cognitive impairment. The superior performance of PSMD over conventional MRI markers results from the combination of DTI, skeletonization of white

matter tracts, and histogram analysis. DTI is a quantitative method that is particularly well suited to characterize microstructural integrity. In contrast, lesion volumes (WMH or lacunes) rely on binary segmentations of non-quantitative images. Hence, lesion volumes disregard gradual differences in tissue damage found in SVD.<sup>35</sup> In addition, DTI measures are more sensitive in capturing SVD-related changes as evidenced by altered DTI measures in white matter appearing normal on conventional imaging.<sup>14,36</sup> Previous studies found DTI parameters to correlate with cognitive performance both cross-sectionally<sup>14,15,37</sup> and over time,<sup>4,38</sup> and in most studies DTI measures were found to correlate with cognitive scores independent of conventional SVD markers. However, one study found DTI to add little on top of brain and lesion volumes.<sup>39</sup> Histogram analysis is a simple, sensitive, and robust way to quantify diffuse pathological changes, as it captures the distribution of diffusivity values across the whole brain.<sup>16</sup> Studies have already shown that histogram measures (such as peak height) can capture disease burden in SVD and correlate with cognition both cross-sectionally<sup>37</sup> and in longitudinal studies.<sup>40,41</sup> However, an unresolved issue was the prominent contamination of whole brain MD data through CSF. Skeletonization overcomes this problem by focusing on the main fiber tracts.<sup>42</sup> Nonetheless, residual CSF contamination can be found in certain parts of the skeleton, such as the fornix.<sup>43</sup> We therefore applied a custom mask to remove these areas from the skeleton. This procedure efficiently

**TABLE 3. Sample Size Estimation for a Hypothetical Clinical Trial of 1.5-Year Duration**

Factor	Treatment Effect Size		
	30%	20%	10%
PSMD	96	216	859
Whole brain MD peak height	183	410	1,636
Normalized WMH volume	258	580	2,315
BPF	4,511	10,149	40,592
Speed score	5,387	12,119	48,471
Normalized lacune volume	11,354	25,545	102,176

BPF = brain parenchymal fraction; MD = mean diffusivity; PSMD = peak width of skeletonized MD; WMH = white matter hyperintensity.

eliminates the CSF peak in the histogram as a prerequisite to calculating the peak width. As a result, PSMD outperforms traditional MD histogram measures (such as whole brain MD peak height) in terms of the association with processing speed, sample size estimates, and interscanner reproducibility.

We found samples with the same diagnosis but recruited through different studies to have remarkably similar PSMDs. This specifically applies to healthy controls from VASCAMY and ADNI, and to population-based elderly subjects from the ASPFS (see Fig 4). The stability of this marker across studies might again relate to the quantitative nature of DTI. Furthermore, it has already been suggested that DTI parameters in general<sup>44</sup> and MD histogram metrics in particular<sup>45</sup> are largely reproducible across different scanners and sequences. Although we cannot fully exclude an influence of scanner type, field strength, and different software versions on MD values,<sup>46</sup> our interscanner reproducibility study using 2 scanners with different field strengths showed the best reproducibility for PSMD. It is plausible that PSMD is less prone to interscanner and interstudy differences than other DTI (histogram) parameters, because peak width does not depend on absolute MD values but rather on the distribution pattern of the histogram.

The comparison with healthy controls and patients with AD pathology (ADNI sample) suggests a strong link between our new marker and SVD. PSMD values in MCI patients with a low WMH load and in demented subjects with a low WMH load were not significantly different from healthy controls. However, subgroups with high WMH load showed increases in PSMD. This suggests that also in AD patients, PSMD mostly captures the SVD-related alterations and not primary neurodegenerative pathology. Given the frequent co-occurrence of AD and SVD in the elderly, tools that allow disentangling the vascular contribution to disease burden are of great interest.<sup>47</sup> Our results suggest that PSMD may serve that purpose.

An important application of PSMD might be the use as a marker for treatment response in clinical trials. The longitudinal analysis with sample size estimations supports this view, as PSMD had the smallest sample size estimate among all variables. Although the longitudinal analysis was limited to CADASIL subjects, comparing our results with a recent study in sporadic SVD patients suggests good generalizability.<sup>48</sup> In line with our analysis, the previous study demonstrated that WMH volume and whole brain MD peak height were able to reduce the required sample size in clinical trials. Our results extend these findings by demonstrating that PSMD can reduce the sample size even further. Moreover, the excellent

interscanner reproducibility suggests that PSMD might be particularly suited for multicenter trials.

A major strength of this study is the validation approach involving multiple large samples. These samples were recruited through different settings and covered a broad spectrum of SVD severity. Each study had a prospective design with standardized MRI and comprehensive clinical examination. Also, major conventional MRI markers were obtained for all samples with SVD. This enabled us to determine the relative importance of our new marker in 4 independent studies. Another strength is the focus on a robust and easy-to-implement marker, which should greatly facilitate implementation in future studies. The processing pipeline is provided online at [www.psm-d-marker.com](http://www.psm-d-marker.com). Given the simple processing steps involved, it is possible to perform the calculation on scanner software directly after image reconstruction within minutes and without any manual intervention.

Our study also has limitations. The use of data from different studies resulted in some differences in scanner field strength, DTI b-values (ranging from 900 to 1,200s/mm<sup>2</sup>), and neuropsychological tests utilized to assess processing speed. Also, there were slight differences in the protocols used for calculating conventional imaging markers and for preprocessing of DTI data. These differences limit comparisons between samples. However, they can also be regarded as a strength. Our findings illustrate the robustness of PSMD under different settings. RUN DMC patients were on average relatively young and mildly affected, which might limit the generalizability of our findings to older cohorts at later stages of the disease. However, patients with later disease stages were included in the memory clinic sample. A potential limitation for the future application of PSMD is that the co-occurrence of large, non-SVD lesions (eg, territorial infarcts or tumors) might impede the automatic calculation of PSMD, as they would have to be manually excluded from the analysis. However, such pathologies are rare in SVD patients, and accordingly they were absent in all our samples. Another limitation is the mainly cross-sectional design. To strengthen our results, we chose advanced statistical methods, such as model decomposition, and included multiple validation samples. Nevertheless, the sensitivity of PSMD in capturing disease progression can only be determined by longitudinal studies. More detailed follow-up studies are needed to determine the value of PSMD as a prognostic marker and to further explore its use as a surrogate marker in clinical trials.

In conclusion, this study presents a novel imaging marker, which we consider to be a major step forward in SVD research. We expect the marker to be of great

utility for research studies and potentially also for clinical use.

## Acknowledgment

This study was funded by the Ludwig-Maximilians-University FöFoLe program (808), the Else Kröner-Fresenius-Stiftung (2014\_A200), and the Vascular Dementia Research Foundation. M.E. received funding from the European Commission (PCIG12-GA-2012-334259). F.-E.d.L. is supported by the Netherlands Organization for Scientific Research (016.126.351). The research of G.J.B. and the Utrecht VCI Study group is supported by grant 2010T073 from the Dutch Heart Association and Vidi grant 91711384 from ZonMw, the Netherlands Organization for Health Research and Development. M.Di. is supported by ERA-NET NEURON within the Sixth European Union Framework Program (01 EW1207). Part of this project was funded through the ADNI (NIH U01 AG024904 and Department of Defense W81XWH-12-2-0012). ADNI is funded by the NIH National Institute on Aging and the NIH National Institute of Biomedical Imaging and Bioengineering. Private sector contributions are facilitated by the Foundation for the National Institutes of Health ([www.fnih.org](http://www.fnih.org)). A list of industry contributions can be found here: <http://adni.loni.usc.edu/about/funding/>.

## Author Contributions

Study concept and design: E.B., M.Du.; data acquisition and analysis: all authors; drafting the manuscript and figures: E.B., M.Du.

## Potential Conflicts of Interest

Nothing to report.

## References

- Pantoni L. Cerebral small vessel disease: from pathogenesis and clinical characteristics to therapeutic challenges. *Lancet Neurol* 2010;9:689–701.
- Wardlaw JM, Smith EE, Biessels GJ, et al. Neuroimaging standards for research into small vessel disease and its contribution to ageing and neurodegeneration. *Lancet Neurol* 2013;12:822–838.
- Wardlaw JM, Valdés Hernández MC, Muñoz-Maniega S. What are white matter hyperintensities made of? Relevance to vascular cognitive impairment. *J Am Heart Assoc* 2015;4:001140.
- Nitkunan A, Barrick TR, Charlton RA, et al. Multimodal MRI in cerebral small vessel disease: its relationship with cognition and sensitivity to change over time. *Stroke* 2008;39:1999–2005.
- Patel B, Markus HS. Magnetic resonance imaging in cerebral small vessel disease and its use as a surrogate disease marker. *Int J Stroke* 2011;6:47–59.
- Duering M, Zieren N, Herve D, et al. Strategic role of frontal white matter tracts in vascular cognitive impairment: a voxel-based lesion-symptom mapping study in CADASIL. *Brain* 2011;134(pt 8):2366–2375.
- Viswanathan A, Godin O, Jouvent E, et al. Impact of MRI markers in subcortical vascular dementia: a multi-modal analysis in CADASIL. *Neurobiol Aging* 2010;31:1629–1636.
- Frisoni GB, Fox NC, Jack CR, et al. The clinical use of structural MRI in Alzheimer disease. *Nat Rev Neurol* 2010;6:67–77.
- De Guio F, Reyes S, Duering M, et al. Decreased T1 contrast between gray matter and normal-appearing white matter in CADASIL. *AJNR Am J Neuroradiol* 2014;35:72–76.
- O'Sullivan M, Jouvent E, Saemann PG, et al. Measurement of brain atrophy in subcortical vascular disease: a comparison of different approaches and the impact of ischaemic lesions. *Neuroimage* 2008;43:312–320.
- Smith EE, Schneider JA, Wardlaw JM, Greenberg SM. Cerebral microinfarcts: the invisible lesions. *Lancet Neurol* 2012;11:272–282.
- Charidimou A, Werring DJ. Cerebral microbleeds and cognition in cerebrovascular disease: an update. *J Neurol Sci* 2012;322:50–55.
- Nucifora PGP, Verma R, Lee S-K, Melhem ER. Diffusion-tensor MR imaging and tractography: exploring brain microstructure and connectivity. *Radiology* 2007;245:367–384.
- Van Norden AGW, De Laat KF, Van Dijk EJ, et al. Diffusion tensor imaging and cognition in cerebral small vessel disease: the RUN DMC study. *Biochim Biophys Acta* 2012;1822:401–417.
- Tuladhar AM, van Norden AGW, de Laat KF, et al. White matter integrity in small vessel disease is related to cognition. *Neuroimage Clin* 2015;7:518–524.
- Tofts PS, Davies GR, Dehmshki J. Histograms: measuring subtle diffuse disease. In: Tofts P, ed. *Quantitative MRI of the brain*. Chichester, UK: John Wiley & Sons, 2003:581–610.
- Duering M, Csanadi E, Gesierich B, et al. Incident lacunes preferentially localize to the edge of white matter hyperintensities: insights into the pathophysiology of cerebral small vessel disease. *Brain* 2013;136(pt 9):2717–2726.
- Tombaugh TN. Trail Making Test A and B: normative data stratified by age and education. *Arch Clin Neuropsychol* 2004;19:203–214.
- van Norden AG, de Laat KF, Gons RA, et al. Causes and consequences of cerebral small vessel disease. The RUN DMC study: a prospective cohort study. Study rationale and protocol. *BMC Neurol* 2011;11:29.
- van der Elst W, van Boxtel MPJM, van Breukelen GJP, Jolles J. The Concept Shifting Test: adult normative data. *Psychol Assess* 2006;18:424–432.
- van der Elst W, van Boxtel MPJ, van Breukelen GJP, Jolles J. Assessment of information processing in working memory in applied settings: the paper and pencil memory scanning test. *Psychol Med* 2007;37:1335–1344.
- Aalten P, Ramakers IH, Biessels GJ, et al. The Dutch Paresnoer Institute—Neurodegenerative diseases; methods, design and baseline results. *BMC Neurol* 2014;14:1–8.
- Petersen RC. Mild cognitive impairment as a diagnostic entity. *J Intern Med* 2004;256:183–194.
- Ghadery C, Pirpamer L, Hofer E, et al. R2\* mapping for brain iron: associations with cognition in normal aging. *Neurobiol Aging* 2015;36:925–932.
- Smith SM, Jenkinson M, Woolrich MW, et al. Advances in functional and structural MR image analysis and implementation as FSL. *Neuroimage* 2004;23(suppl 1):S208–S219.
- Zwiers MP. Patching cardiac and head motion artefacts in diffusion-weighted images. *Neuroimage* 2010;53:565–575.
- Smith SM, Jenkinson M, Johansen-Berg H, et al. Tract-based spatial statistics: voxelwise analysis of multi-subject diffusion data. *Neuroimage* 2006;31:1487–1505.

28. R Core Team. A language and environment for statistical computing. Vienna, Austria: R Foundation for Statistical Computing, 2014.
29. Decarli C, Maillard P, Fletcher E. Four Tissue Segmentation in ADNI II. 2013. Available at: [https://www.alz.washington.edu/WEB/adni\\_proto.pdf](https://www.alz.washington.edu/WEB/adni_proto.pdf). Accessed Feb 5, 2016
30. Otsu N. A threshold selection method from gray level histogram. *IEEE Trans Syst Man Cybern* 1979;9:62–66.
31. Fox J, Weisberg S. An {R} Companion to Applied Regression, Second Edition. Thousand Oaks CA: Sage, 2011. Available at: <http://socserv.socsci.mcmaster.ca/jfox/Books/Companion>. Accessed Feb 5, 2016.
32. Lindeman RH, Merenda PF, Gold RZ. Introduction to bivariate and multivariate analysis. Glenview, IL: Scott Foresman and Company, 1980.
33. Grömping U. Relative importance for linear regression in R: the package relaimpo. *J Stat Softw* 2006;17:139–147.
34. Faul F, Erdfelder E, Lang A-G, Buchner A. G\*Power 3: a flexible statistical power analysis program for the social, behavioral, and biomedical sciences. *Behav Res Methods* 2007;39:175–191.
35. Maillard P, Fletcher E, Harvey D, et al. White matter hyperintensity penumbra. *Stroke* 2011;42:1917–1922.
36. De Groot M, Verhaaren BFJ, De Boer R, et al. Changes in normal-appearing white matter precede development of white matter lesions. *Stroke* 2013;44:1037–1042.
37. Lawrence AJ, Patel B, Morris RG, et al. Mechanisms of cognitive impairment in cerebral small vessel disease: multimodal MRI results from the St George’s cognition and neuroimaging in stroke (SCANS) study. *PLoS One* 2013;8:e61014.
38. Jokinen H, Schmidt R, Ropele S, et al. Diffusion changes predict cognitive and functional outcome: the LADIS study. *Ann Neurol* 2013;73:576–583.
39. van Norden AGW, van Uden IWM, de Laat KF, et al. Cognitive function in small vessel disease: the additional value of diffusion tensor imaging to conventional magnetic resonance imaging: the RUN DMC study. *J Alzheimers Dis* 2012;32:667–676.
40. Holtmannspotter M, Peters N, Opherck C, et al. Diffusion magnetic resonance histograms as a surrogate marker and predictor of disease progression in CADASIL: a two-year follow-up study. *Stroke* 2005;36:2559–2565.
41. Molko N, Pappata S, Mangin JF, et al. Monitoring disease progression in CADASIL with diffusion magnetic resonance imaging: a study with whole brain histogram analysis. *Stroke* 2002;33:2902–2908.
42. Metzler-Baddeley C, O’Sullivan MJ, Bells S, et al. How and how not to correct for CSF-contamination in diffusion MRI. *Neuroimage* 2012;59:1394–1403.
43. Berlot R, Metzler-Baddeley C, Jones DK, O’Sullivan MJ. CSF contamination contributes to apparent microstructural alterations in mild cognitive impairment. *Neuroimage* 2014;92:27–35.
44. Grech-Sollars M, Hales PW, Miyazaki K, et al. Multi-centre reproducibility of diffusion MRI parameters for clinical sequences in the brain. *NMR Biomed* 2015;28:468–485.
45. Cercignani M, Bammer R, Sormani MP, et al. Inter-sequence and inter-imaging unit variability of diffusion tensor MR imaging histogram-derived metrics of the brain in healthy volunteers. *Am J Neuroradiol* 2003;24:638–643.
46. Gunda B, Porcher R, Duering M, et al. ADC histograms from routine DWI for longitudinal studies in cerebral small vessel disease: a field study in CADASIL. *PLoS One* 2014;9:e97173.
47. Prins ND, Scheltens P. White matter hyperintensities, cognitive impairment and dementia: an update. *Nat Rev Neurol* 2015;11:157–165.
48. Benjamin P, Zeestraten E, Lambert C, et al. Progression of MRI markers in cerebral small vessel disease: sample size considerations for clinical trials. *J Cereb Blood Flow Metab* 2016;36:228–240.